ENGINEERING & DEVELOPMENT GROUP
ISRAEL AEROSPACE INDUSTRIES LTD

A REVIEW OF AERONAUTICAL FATIGUE INVESTIGATIONS IN ISRAEL

(April 2007 – March 2009)

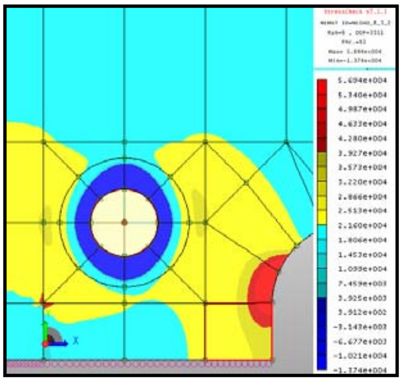

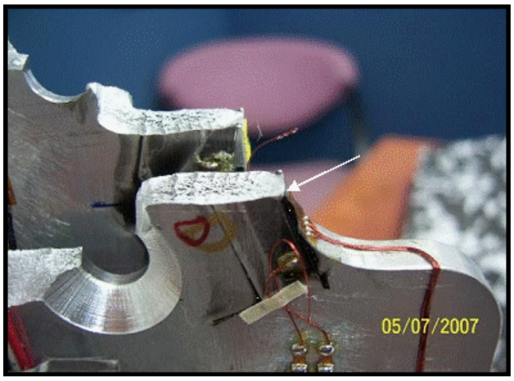

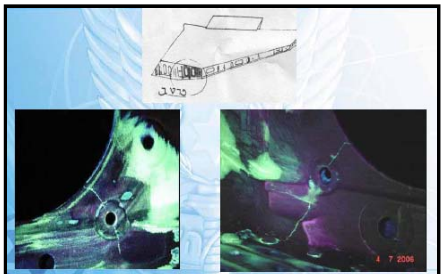
A-4 front spar cracking

Compiled by:
Abraham Brot
Engineering Division
Israel Aerospace Industries
Ben-Gurion Airport, Israel

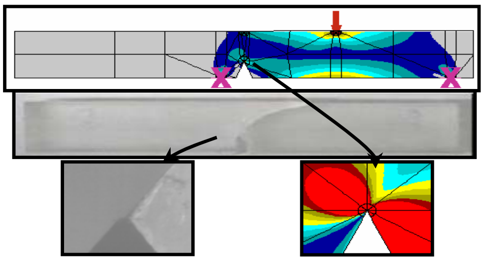

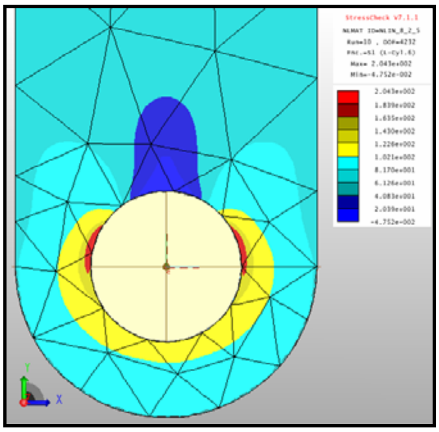

Presented at the 31st Conference of the International Committee on Aeronautical Fatigue (ICAF)
Rotterdam, Netherlands
26 May 2009

A REVIEW OF AERONAUTICAL FATIGUE INVESTIGATIONS IN ISRAEL

APRIL 2007 – MARCH 2009

Compiled by:
Abraham Brot
Engineering Division
Israel Aerospace Industries
Ben-Gurion Airport, Israel

abrot@iai.co.il

SUMMARY

This review summarizes fatigue and fracture-mechanics investigations that were performed in Israel during the period April 2007 to March 2009. The review includes contributions from Israel Aerospace Industries Ltd. (IAI), Israel Air Force (IAF), Tel-Aviv University (TAU), Ben-Gurion University (BGU) and the Hebrew University of Jerusalem.

Presented at the 31st ICAF Conference
Rotterdam, Netherlands
26 May 2009

TABLE OF CONTENTS

A REVIEW OF AERONAUTICAL FATIGUE INVESTIGATIONS IN ISRAEL APRIL 2007 – MARCH 2009

11.1 INTRODUCTION

The Israel National Review summarizes work performed in the field of aeronautical fatigue in Israel during the period April 2007 to March 2009. The previous National Review [1] covered aeronautical fatigue activities up to March 2007. The following organizations contributed to this review:

Israel Aerospace Industries Ltd. (IAI)
Israel Air Force (IAF)
Tel-Aviv University (TAU)
Ben-Gurion University (BGU)
Hebrew University of Jerusalem (HUJI)

The National Review was compiled by Abraham Brot of IAI (abrot@iai.co.il).

11.2 FATIGUE ANALYSIS, TESTING AND LIFE EXTENSION

11.2.1 Residual Tensile Stresses Induced by Cold-Working a Fastener Hole (C. Matias, Y. Freed and A. Brot, IAI)

The Israel National Review from the ICAF 2007 Conference described a crack that initiated at a notched edge near a cold-worked fastener hole and propagated towards the hole during a spectrum component fatigue test [1].

Fractographic analysis confirmed that the crack initiated at the edge and grew towards the hole. Since the maximum measured stress in the notch was not sufficiently high to explain crack-initiation during the test, it was suspected that the tensile residual stresses at the edge contributed to the cracking. An experimental study was initiated in order to measure the tensile residual stresses induced by cold working at various edges located near cold-worked holes. Tensile residual stresses as high as 35 ksi were measured at an edge near a cold-worked hole. Elastic-plastic finite-element analysis results (ABAQUS and StressCheck) showed good agreement with the experimental results. Fatigue analysis has shown that when these residual stresses are combined with high cyclic notch stresses that arise from external loading, the fatigue life at the edge can be drastically reduced.

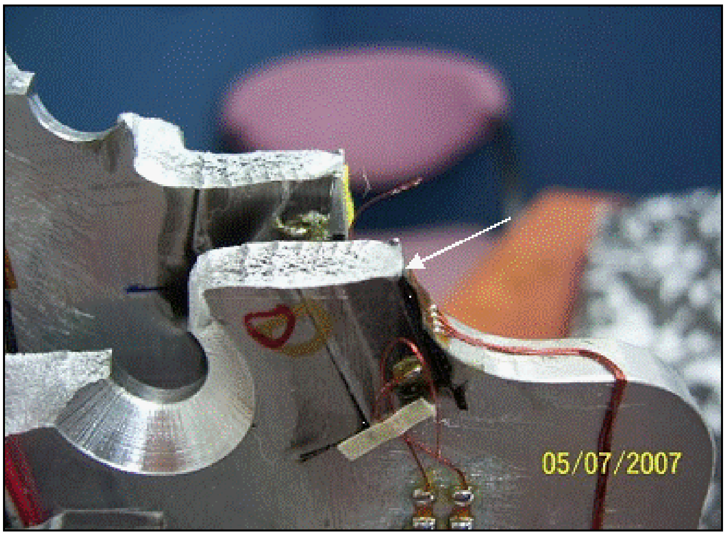

Figure 1: Failure of the Specimen with the Failure Originating from the Notch Radius (as shown)

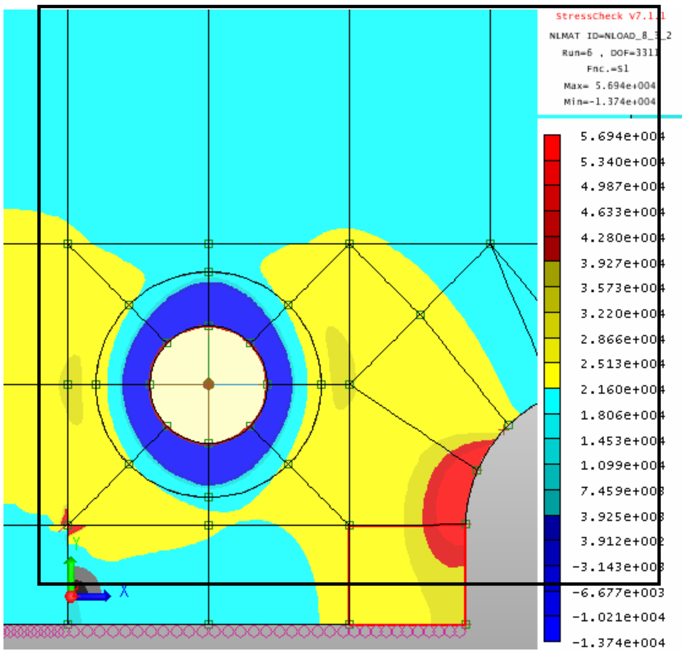

Figure 2: Elastic-Plastic StressCheck Results for a Cold-Worked Hole under a 20 ksi Remote Stress

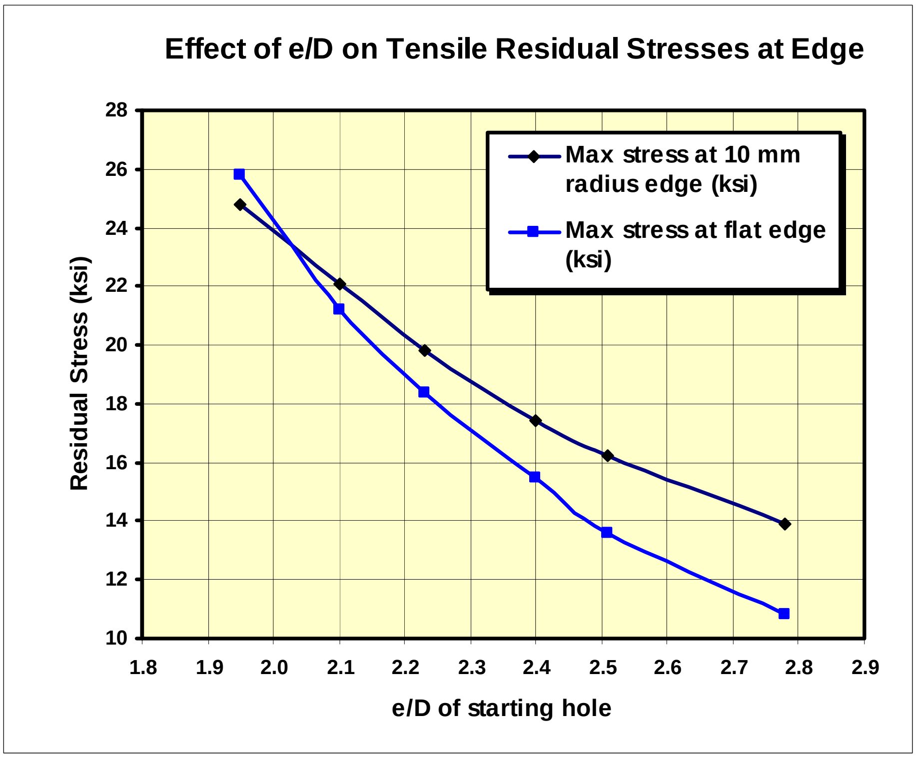

Figure 3: Tensile Residual Stresses Induced by Cold-Working as a Function of Edge-Distance (Based on StressCheck FEM Results)

When the stress-concentration at the notched-edge was reduced, by increasing the notch radius, the fatigue life was significantly increased and the crack initiated from the outer edge of the countersink, where the influence of the cold-working was minimal. A 3D StressCheck model confirmed this result.

Preliminary results were presented at the 47th Israel Annual Conference on Aerospace Sciences [2]. More detailed results were presented at the 2007 ASIP Conference [3].

11.2.2 Stress-Distributions in Lugs Having Interference-Fit Bushings (Y. Freed, A. Brot, IAI)

Interference-fit bushings are often installed in lugs in order to increase their fatigue lives. A specific lug made from 4340 steel was the topic of an ongoing investigation which is being conducted with the aid of elastic-plastic StressCheck finite-element models. The aim of the study is to vary specific parameters and calculate the resulting local stress-range at the lug bore. *(Stress-range can be considered a measure of the criticality of the lug in fatigue.)* Comparative fatigue lives are then calculated using strain-life software. Among the parameters that were varied are the degree of interference-fit, the applied load and the bushing thickness. The loading was kept in the lug longitudinal direction with R = -1 in all cases. In time, the investigation will be broadened to include oblique loading and additional R-ratios. Figure 4 shows the maximum principal stresses on a lug having a 0.4% bushing interference and a 100 ksi bearing stress. Figure 5 describes the effect of bushing interference on the local stress-range. The results of Figure 5 clearly show how the bushing interference significantly reduces the local stress-range.

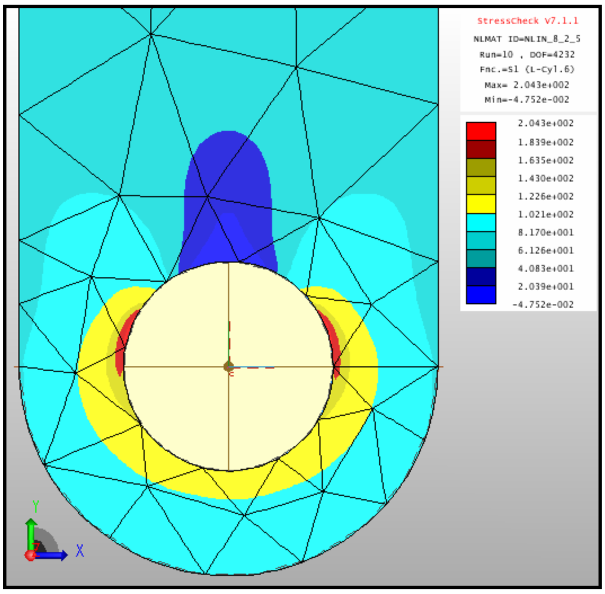

Figure 4: StressCheck FEM for a 0.4% Bushing Interference with 100 ksi Bearing Stress

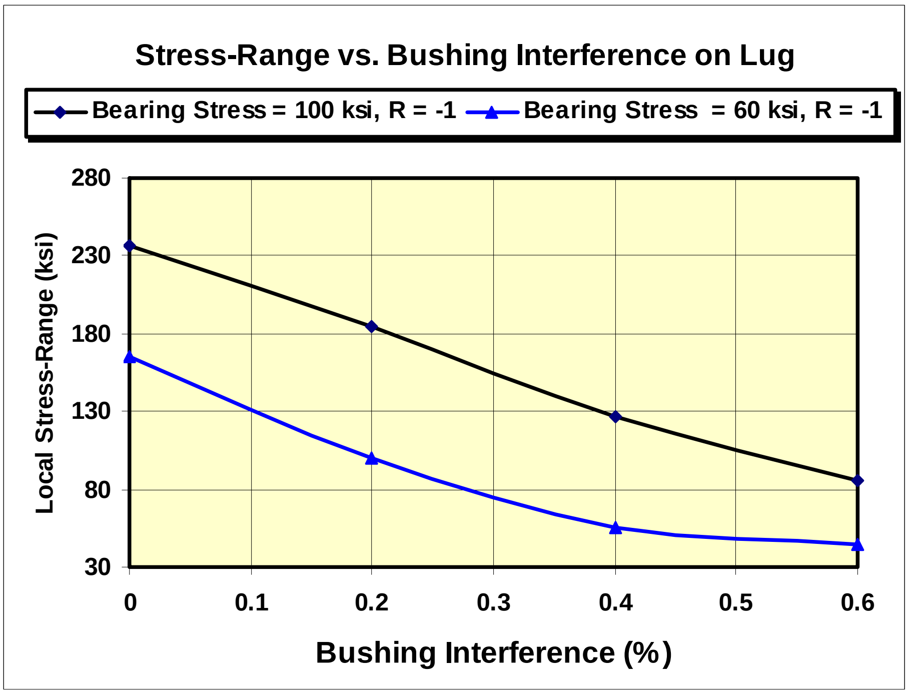

Figure 5: Effect of Bushing Interference on the Local Stress Range

11.2.3 Autofrettaged Thick-Walled Cylinders and Spherical Vessels (M. Perl et al, Ben-Gurion University)

Autofrettage of large diameter tubes (gun barrels) is used to increase the elastic strength of the tube and to increase its fatigue life. It is based on the permanent expansion of the cylinder bore using either hydraulic pressure or an oversize mandrel. The theoretical solution of the autofrettage problem involves different yield criteria, the Bauschinger effect and the recalculation of the residual stress field after machining. Accurate stress-strain data is needed for the numerical analysis of the residual stress field due to autifrettage. Although this topic does not relate directly to aeronautical fatigue, it was included in this review because of the similarity of the autofrettage process to that of the cold-working process that is used extensively in aircraft structures. This research is a direct continuation of previous work presented in the 2007 Israel National Review [1].

A method dealing with the thermal simulation of an arbitrary residual stress field in an autofrettaged thick-walled spherical pressure vessel is described in [4]. The equivalent thermal load was previously shown to be the only feasible method by which the residual stresses due to autofrettage and its redistribution, as a result of cracking, can be implemented in a finite element (FE) analysis of a fully or partially autofrettaged thick-walled cylindrical pressure vessel. The present analysis involves developing a similar methodology for treating an autofrettaged thick-walled spherical pressure vessel. A general procedure for evaluating the equivalent temperature loading for simulating an arbitrary, analytical or numerical sphero-symmetric autofrettage residual stress field in a spherical pressure vessel is developed. Once presented, the algorithm is applied to two distinct cases. In the first case, an analytical expression for the equivalent thermal loading is obtained for the ideal autofrettage stress field in a spherical shell. In the second case, the algorithm is applied to the discrete numerical values of a realistic autofrettage residual stress field incorporating the Bauschinger effect. As a result, a discrete equivalent temperature field is obtained. Furthermore, a FE analysis is performed for each of the above cases, applying the respective temperature field to the spherical vessel. The induced stress fields are evaluated for each case and then compared to the original stress. The FE results prove that the proposed procedure yields equivalent temperature fields that in turn simulate very accurately the residual stress fields for both the ideal and the realistic autofrettage cases.

The influence of the Bauschinger effect (BE) on the three dimensional, Mode I, combined stress intensity factor (SIF) distributions for arrays of longitudinal coplanar, surface cracks emanating from the bore of a fully or partially autofrettaged thick-walled cylinder was investigated [5]. The combined SIFs, K_{IN}, that depend on pressure effects and the "realistic"– Bauschinger effect dependent autofrettage (BEDA), or, that depend on pressure effects and the "ideal" – Bauschinger effect independent autofrettage (BEIA), are obtained and compared for crack depth to wall thickness, a/t = 0.01- 0.25; crack ellipticity, a/c=0.5 - 1.5; crack spacing ratio, 2c/d=0.25 - 0.75; and autofrettage level, e =30%, 60% and 100%. The 3D analysis is performed via the finite element method and the submodeling technique, employing singular elements along the crack front. Both autofrettage residual stress fields, BEDA and BEIA, are simulated using an equivalent temperature field. The combined SIF; K_{IN}, is found to vary along the crack front with the maximum determined by the crack ellipticity, crack depth, and crack spacing ratio. For a partially autofrettaged cylinder; the influence of the BE on the combined SIF, K_{IN}, is substantially reduced as the level of overstrain becomes smaller. For some cases, when comparing like crack distributions, the K_{IN} values obtained from the BEDA model are found to be as much as 100% higher than the K_{IN} values that are computed using the BEIA model. A pressurized thick-walled cylinder with BEDA can be most critical when small cracks are farther apart. As crack depth increases, or when the spacing between cracks is smaller, the SIFs increase. Though the differences in the BEDA SIF, K_{IA}, between e = 100% and 60% are small (7 - 15%, in most cases), the increased level of autofrettage produces a 23 - 30% decrease in the combined SIF values, K_{IN}. 1n certain cases, the BEIA model implies an infinite fatigue life, whereas the BEDA model for the same parameters implies a finite life. Therefore, it is important to perform a full 3D analysis to determine the real life cycle of the pressurized cylinder for materials that exhibit the BE.

The Bauschinger effect on internal surface cracks was investigated in [6]. Networks of radial and longitudinally-coplanar, internal, surface cracks are typical in rifled, autofrettaged, gun barrels. In two previous papers, the separate effects of large arrays of either radial or longitudinally-coplanar semi-elliptical, internal, surface cracks in a thick-walled, cylindrical, pressure vessel under both ideal and realistic autofrettage were studied. When pressure is considered solely, radial crack density and longitudinal crack spacing were found to have opposing effects on the prevailing stress intensity factor, K_{IP}. Furthermore, the addition of the negative stress intensity factor (SIF), K_{IA}, resulting from the residual stress field due to autofrettage, whether ideal or realistic, tended to decrease the combined SIF $K_{IN} = K_{IP} - |K_{IA}|$. Therefore, to assess the fracture endurance and the fatigue life of a cylindrical, autofrettaged, pressure vessel containing such a network of cracks, it is necessary to determine the K_{IA}'s and the K_{IN}'s. This investigation presented the K_{IA} and the K_{IN} distribution for numerous configurations of semi-circular and semi-elliptical, crack networks affected by pressure and autofrettage. The 3-D analysis is performed via the finite element (FE) method and the submodeling technique, employing singular elements along the crack front and the various symmetries of the problem. The networks considered included up to 128 equally spaced cracks in the radial direction; with relative, longitudinal crack spacing, 2c/d, from 0.1 to 0.99; covered autofrettage level of 100 percent; employed a wide range of crack depth to wall thickness ratios, a/t, from 0.01 to 0.4; and, involved cracks with various ellipticities of crack depth to semi-crack length, a/c, from 0.2 to 2. The results clearly indicate that the combined SIFs are considerably influenced by the three-dimensionality of the problem and the Bauschinger effect to such an extent that cracks predicted closed by the ideal Autofrettage model are predicted as remaining open by the realistic autofrettage model. In addition, the SIFs are found to depend upon the other parameters enumerated previously, namely: radial crack density, longitudinal crack spacing, crack depth, crack ellipticity, and the autofrettage level.

Another study dealt with constructing a 3-D model for evaluating the residual stress field due to swage Autofrettage [7]. In order to maximize the performance of' modern gun barrels in terms of strength-to-weight ratio and total fatigue life, favorable compressive residual stresses are introduced to the inner portion of the barrel, commonly by the autofrettage process. There are two major autofrettage processes for overstraining the tube: the hydrostatic and the swage. There are several theoretical solutions for hydrostatic autofrettage based on Lame's solution and the von Mises or Tresca yield criteria. The residual stress field due to hydraulic autofrettage is treated as an axisymmetric two-dimensional problem solved in terms of the radial displacement solely. Once the Bauschinger effect was included in these models they yield very realistic results. Unlike in the case of hydraulic autofrettage, swage autofrettage needs to be modeled by a three-dimensional model. The present analysis suggests a new .3-D axisvmmetric model for solving the residual stress field due to swage autofrettage in terms of both the radial and the axial displacements. The axisymmetric equilibrium equations are approximated by finite-differences and solved then by Gauss-Seidel method. Using the new computer code the stresses, strains, displacements, and forces are determined. A full-scale instrumented swage autofrettage test was conducted and the numerical results were validated against the experimental findings. The calculated strains, the permanent bore enlargement, and the mandrel pushing force were found to be in very good agreement with the measured values.

11.2.4 Fatigue of an Access Panel Cutout Having Satellite Holes (C. Matias and A. Brot, IAI)

Access panels in aircraft are sometimes designed with satellite holes around the cutout, used to secure the panel cover. Cracking will often occur, starting from the satellite holes, due to their high local stresses. These high local stresses are the result of the proximity of the satellite holes to the cutout. The problem is likely to be even more severe if there are nut-plate rivet holes close to the edge of the cutout. A possible way to alleviate the cracking problem is to cold-work all the satellite holes.

A component test program is being performed at IAI in order to investigate the problem and to evaluate several solutions. Testing is being performed on 7457-T7351 aluminum panels having overall dimensions of 900 x 480 mm. The nominal panel thickness is 5.4 mm. The panel cutout has a diameter of 120 mm, with the general configuration shown in Figure 6.

The panel is being loaded to a typical flight-by-flight randomized wing gust and maneuver spectrum having approximately 18 cycles per flight and having a maximum stress of 19.6 ksi (135 MPa).

Two panel configurations are currently being tested: (1) panel with satellite holes, as shown in Figure 6; (2) The panel shown in Figure 6 with all satellite holes cold-worked.

Strain-gages have been installed on both faces of each panel, and crack-propagation gages (CPGs) will be used to detect crack-initiation at the satellite holes. Strain-gage readings are taken every 5000 flights, and NDI will be performed if anomalous strain-gage readings are encountered or if the CPGs indicate crack-initiation.

Figure 7 shows a strain-gaged test panel installed in the test fixture. After completion of the current test program, other solutions may also be evaluated.

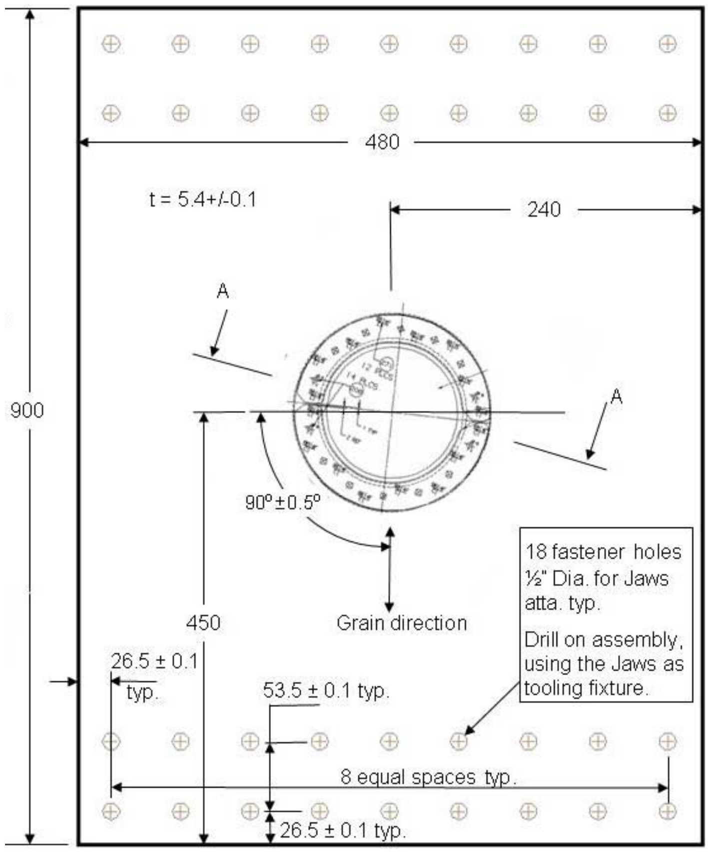

Figure 6: Test Panel Configuration

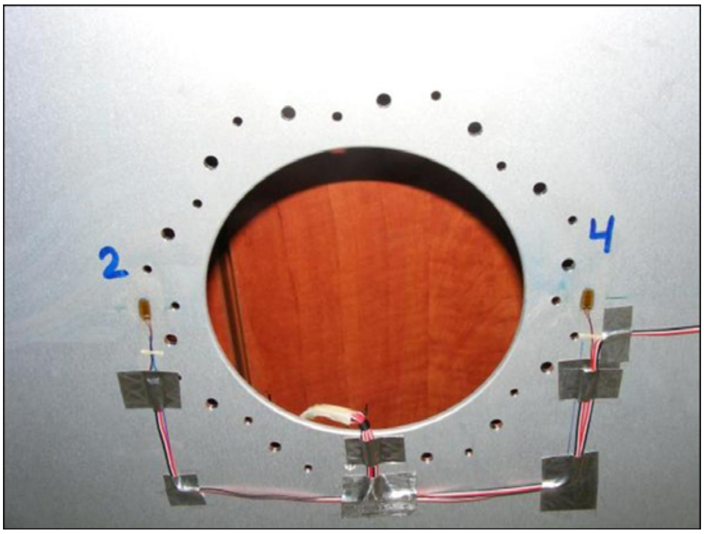

Figure 7: Test Panel Installed in Test Fixture

11.2.5 G150 Executive Jet Full-Scale Fatigue Test (A. Alperovich, IAI)

As part of the damage-tolerance certification, a G150 test-article was tested for two lifetimes (40,000 flights) of fatigue loading and another half-lifetime (10,000 flights) of damage-tolerance testing. This was reported in the 2007 Israel National Review [1].

The test-article included the fuselage and both wings. The tested areas consisted of the forward fuselage and cabin to the aft pressure bulkhead and fuel tank. Both entire wings were fatigue tested. Since the aft fuselage and empennage have not changed significantly from the G100 model, they were not fatigue tested and acted only as load application elements. Figure 8 is a photograph of the G150 full-scale fatigue test.

Figure 8: G150 Executive Jet Full-Scale Fatigue Test

The damage-tolerance testing (10,000 flights) took place between May 2007 and March 2008. Some additional cracks were detected during the damage-tolerance test phase at the aft pressure bulkhead, wings and at the wing carry-through structure.

Some of these cracks were repaired in order to continue the test. Design changes and retrofit solutions for the fleet were analyzed by FEM and checked on a production aircraft. At some locations, where cracking would not endanger the test-article, the cracks were allowed to grow and provide crack growth data as a part of the damage-tolerance testing. Wherever necessary, the cracked locations were strengthened in order to avoid cracking in production aircraft.

During the damage-tolerance testing, 24 artificial flaws (sawcuts) were inflicted in various areas of the test-article. Seven of these flaws grew sufficiently to provide measured crack growth data.

After the end of the damage-tolerance testing, two wing and fuselage residual strength tests were performed. The wing residual strength test was performed with the application of the wing design limit load case and in the presence of two large cracks at two critical locations. The fuselage residual strength test was performed with the application of 10.4 psi cabin pressurization (15% above the normal operating pressure) in the presence of two two-bay cracks and several unrepaired cracks inside the aft pressure bulkhead, which appeared during the fatigue and damage-tolerance tests.

A selected teardown inspection of the tested wing and the fuselage was started during January 2009. After the completion of the teardown inspection, the G150 Continuing Airworthiness Report will be updated as needed, with all the crack findings and crack growth data measured during the full-scale fatigue test.

Figure 9 shows photos of the residual strength testing that was performed.

Figure 9: Residual Strength Testing of the G150 Aircraft. ***(a) wing residual strength test (upper left), (b) crack at wing lower skin access panel (upper right), (c) two-bay fuselage crack, view from inside the fuselage (lower left) and (d) view from outside the fuselage (lower right)***

11.2.6 G250 Executive Jet Fatigue Substantiation Program (A. Hermelin and A. Brot, IAI)

Israel Aerospace Industries and the Gulfstream Aerospace Corporation are currently jointly developing the G250 super mid-size executive jet. The aircraft will have a range of 3,400 nautical miles at a maximum speed of Mach 0.85. It will cruise at altitudes up to 45,000 feet. The first flight of the G250 is scheduled for the second half of 2009. Certification of the G250 to the FAA and EASA regulations is expected to be completed in 2011. Deliveries of the G250 will also begin in 2011. The aircraft is powered by twin Honeywell HTF7250G engines, each producing 7,445 pounds of thrust. The G250 will be capable of nonstop flight from New York to London or from London to Dubai. The aircraft will have a very roomy and quiet cabin. The cabin environment will include 100% fresh air and a cabin altitude not exceeding 7,000 feet.

As part of its damage-tolerance certification program, a structurally complete G250 test-article will be fatigue tested for two lifetimes (40,000 flights) followed by approximately half a lifetime (10,000 flights) of damage-tolerance testing, with artificial flaws inflicted at critical locations. Residual strength tests, under limit loads and cabin pressurization, will be performed in the presence of large cracks at several critical locations. This will be followed by a selected teardown inspection.

The full-scale fatigue test will include lateral loading on the tail and a suitable representation of engine support loading and main landing gear backup structure loading. The loading spectrum is expected to contain approximately 80 cycles per flight. Loads will be applied through 58 loading zones and will be reacted at six locations. A cabin pressure differential of 9.2 psi will be applied during each flight.

In addition to the full-scale fatigue test described above, fatigue and damage-tolerance component tests will be performed for the landing gear, aileron (composite material), spoiler and flap extension system.

Figure 10 shows the G250 design configuration.

Figure 10: G250 Executive Jet Design

11.3 STRUCTURAL INTEGRITY OF COMPOSITE MATERIALS

11.3.1 Comprehensive Structural Integrity of Composites (Z. Granot, IAI and S. Gali, Consultant)

Composite structures must perform their function throughout the projected service life, while conforming to rigorous safety and economic requirements. The structures are subjected to various initial and in-service damage threats and are subjected to a realistic mix of load-time-environment sequences. In the ICAF 2007 National Review [1], an experimental and analytical program on the cumulative damage effects for repetitive loads in composites was discussed. A paper was presented at the ICAF 2005 symposium summarizing IAI's methodology for predicting the fatigue life of composite material structures [8].

Now this program is being expanded and generalized to consider not just repetitive load cycles, but also other factors contributing to the overall damage. The effects of load-time-temperature-moisture sequences including creep loading are all considered as contributing factors, both individually and collectively.

The tasks being considered are:

- Accelerated testing on various coupons and subassemblies, for both static and repetitive loading, and to various load-time-environment sequences
- Development of advanced modeling techniques to model and explain the behavior and failure modes of coupons and subassemblies
- Development and implementation of advanced failure criteria, for initiation, progression and final failure. These should consider static, fatigue, creep, environmental, and residual strength degradation
- Development of trade-off calculations for determining the most optimum materials and design features
- Development of advanced preventative, maintenance, monitoring and inspection techniques to enhance and maintain the structure through its service life

Expected results from the program:

- Accelerated testing techniques and know-how
- Advanced modeling techniques
- Advanced failure criteria and analytical methodology
- Analytical system for parametric trade-off studies
- Optimum design features
- Techniques for slowing degradation and life extension

11.3.2 Bonded Composite Patch Repairs – Analysis and Testing (I. Kressel, IAI, M. Tur, TAU, S. Gali, Consultant)

At the 2005 ICAF Symposium, a poster was presented on the damage tolerance of bonded composite repairs [9]. At the 2007 ICAF Symposium, this work was extended to include the "smart repair concept" [10]. Currently we are in the process of evaluating the environmental effects on both single and double sided bonded repairs. A bonded repair specimen was designed, manufactured and fatigue tested. It consists of a carbon-epoxy, single or double-sided patch, bonded to an aluminum plate (2024-T3, 1.6mm thick). Each patch was made of three plies of Fiberite 753 style 3K-70-P carbon/epoxy and one ply of Fiberite 753 style 120 fiberglass/epoxy prepreg. All specimens were cured under a vacuum at 120°C. A typical specimen is shown in Figure 11. The cure monitoring was performed using embedded fiber-optics Bragg sensors.

Figure 11: Bonded Repair Specimen

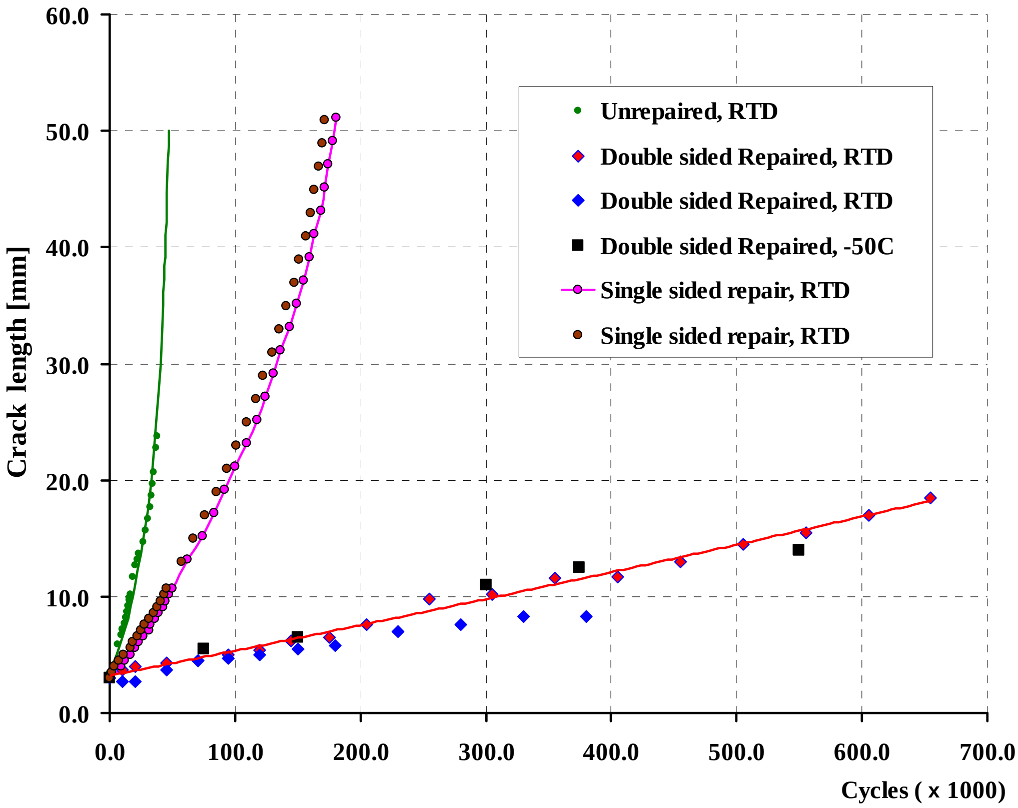

Figure 12: Fatigue Test Results of Bonded Repairs

The test results are presented in Figure 12. It can be seen that double sided repair has the best performance in retarding the crack propagation. In spite of the large difference in thermal expansion coefficient between the carbon patch and the aluminum substrate, no significant change in crack growth rate was observed under test performed both at RTD and -50°C. For the one sided repair, it is clearly seen that the out-of-plane bending reduces the effectively of the patch. Compared to an unrepaired reference specimen, the one sided repair has increased the life by a factor of 4.5. Further tests of one sided carbon repairs under -50°C are scheduled soon.

11.3.3 The Use of Composite Material Strips to Extend the Damage-Tolerance Life of Integrally Stiffened Aluminum Panels, (A. Brot, I Kressel, IAI)

Israel Aerospace Industries (IAI) has studied the damage-tolerance behavior of integrally stiffened metallic structures as part of an international project called **DaToN** *(Innovative Fatigue and **Da**mage **To**lerance Methods for the Application of **N**ew Structural Concepts)*, which was partially funded by the European Commission. IAI has performed both analytical and experimental studies of integrally stiffened metallic structures, in the framework of this project.

As part of the testing and analysis performed, composite material strips were used to enhance the crack growth resistance of the panels. The paper also describes the analytical calculations supporting the experimental results.

In order to improve the performance of a two-stringer integral panel, two 35mm wide strips of AS4/3502 carbon-epoxy were bonded to the panels. Each strip consisted of *three* layers of carbon-epoxy material. The purpose of the strips is to reduce the stress-intensity of a crack that grows under it, thereby increasing the crack growth life of the panel. On an identical panel, two 35mm wide strips of Textron 5521 F/4 boron-epoxy were bonded. Each strip consisted of *two* layers of boron-epoxy material. Both hybrid panels were tested at room temperature.

The results show that both hybrid panels had a significantly slower crack growth rate than the unreinforced panel. The crack growth life of the three-layer carbon-epoxy gave somewhat better results than the two-layer boron-epoxy strips, as is shown in Figure 13.

An additional test was performed with a carbon-epoxy reinforced panel at an ambient temperature of -50°C. The results show that the crack grew *significantly slower at -50°C than at room temperature*, showing that the reduced crack growth rate of aluminum at -50°C was more decisive than the presence of tensile residual stresses.

A NASTRAN finite-element model (FEM) was built to study the effect of the reinforcing strips. The stress-intensity results, obtained from the FEM, were input into NASGRO ver. 5 *(crack growth software)* in order to compute the expected crack growth characteristics.

This experimental and analytical study demonstrated the large potential that exists by use of CFRP or BFRP patches to increase the crack growth life of integrally stiffened aluminum panels. Further testing and analysis is needed to confirm quantitatively these results.

Preliminary results of this study were presented at the 48th Israel Annual Conference on Aeronautical Sciences [11]. The full results will be presented at the 25th ICAF Symposium [12].

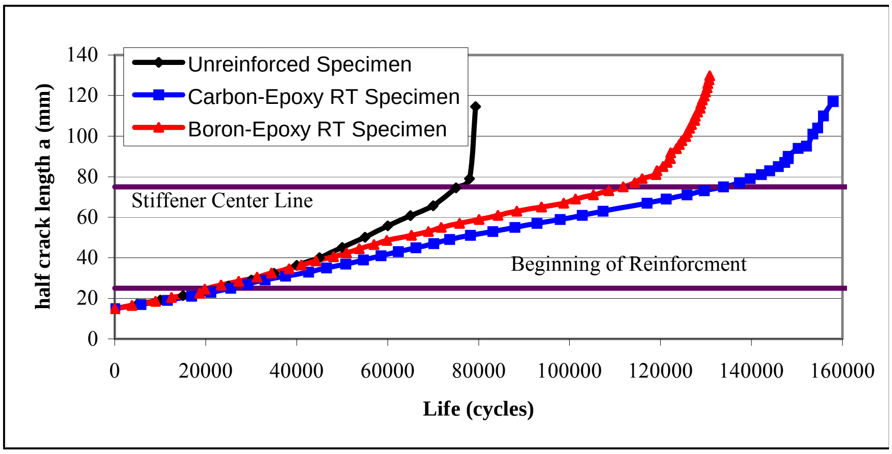

Figure 13: Crack Growth of Both Reinforced Panels and the Unreinforced Two-Stringer Panel

11.3.4 Substantiation of an Airborne Composite Radome Mounted on an Aircraft Dome, (I. Kressel, IAI)

A dome mounted composite structure radome was designed and substantiated for an early warning surveillance system. The substantiation process included development of material design allowables, coupons, element testing and a full scale static test to the maximum ultimate design loads.

The composite radome is a honeycomb structure shell with fiberglass skins. The thickness of the honeycomb and the skins vary according to electrical requirements. The general dimensions of the radome can be seen in Figure 14.

The test program, at a coupon level, provided laminate-level allowable design strain values covering each failure mode and environmental condition. Design allowable values are based on saturated laminates and sandwiches. Effect-of-defects and cyclic loading were also included. Corrections for material variability followed approved procedures in MIL-HDBK-17.

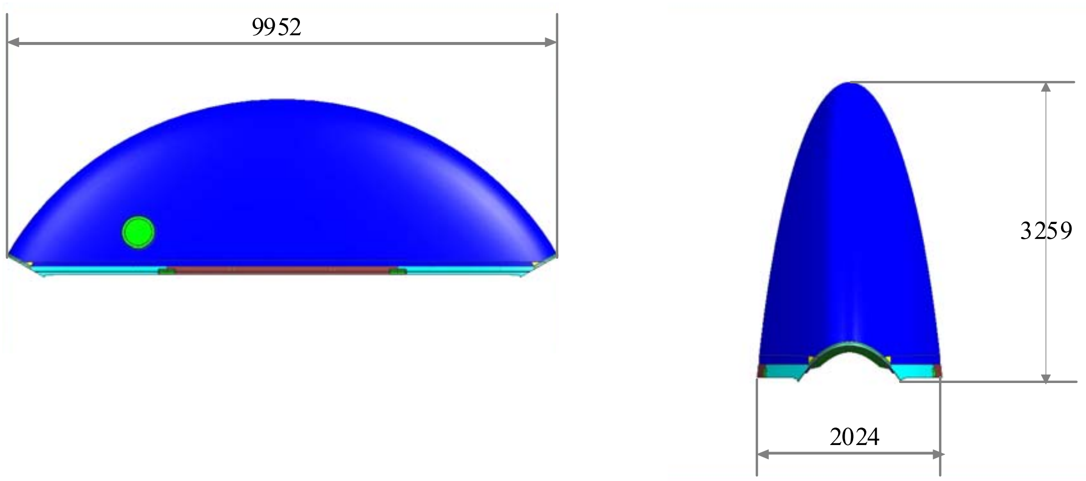

Figure 14: Overall Radome Dimensions (mm)

The two primary damage-tolerance requirements were addressed: damage growth characterization and residual strength-capability. Considering the applied strains, IAI selected a "no-growth" approach for the composite radome. This philosophy states that any damage that is visually undetectable should not become critical. Structure with this type of damage must be capable of carrying ultimate load for the operational life of the airplane. This approach was validated through a series of tests at coupon and component levels. Impact damage was inflicted on a leading edge element specimen at the barely visible level, combined with environmental aging followed by fatigue testing under load cycles representative of twenty (20) design service lifetimes. The leading edge test set-up is shown in Figure 15. Ultrasonic inspection revealed the absence of damage growth. IAI fatigue evaluation of the radome-dome metal splice structure was based on established methods.

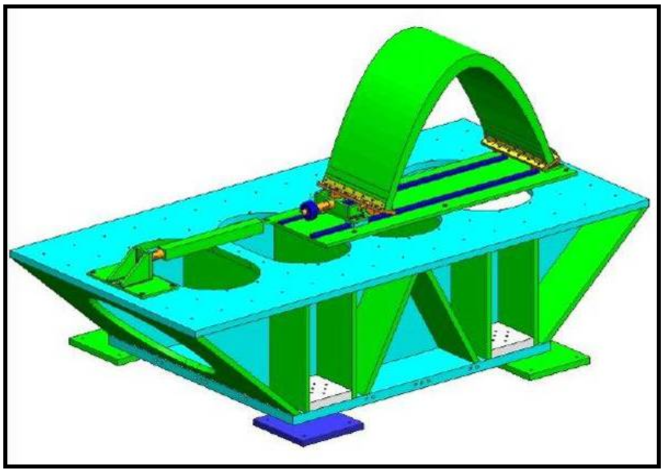

Figure 15: Leading Edge Fatigue Test Set-Up

Full scale limit load strain surveys and ultimate load testing demonstrated the predictive capability of the FEA model. A loads enhancement factor was added in order to compensate for temperature effects. This factor was established by a series of element tests, representing the honeycomb to solid glass interface at the radome root. Since such a radome is manufactured from at least two batches of material, the material properties variation is inherent and therefore an additional knock-up factor is not required.

A summary of this project will be presented at the 25th ICAF Symposium [13].

11.4 PROBALISTIC STUDIES

11.4.1 Risk-Analysis as a Supplement to Damage-Tolerance Analysis (A. Brot, IAI)

Damage-tolerance has been used to substantiate civilian and military aircraft structures for fatigue life for more than 30 years. For the most part, the damage-tolerance approach has proved to be successful in avoiding fatigue failures.

At times, aircraft must be inspected earlier, or more often than planned, due to fatigue test findings or changes to the operating mission-mix or loading spectrum. This can be very *expensive to the customer*, and can have a *severe effect on aircraft availability.*

Risk-analysis, based on probabilistic considerations, can be used to determine the risk of a fatigue failure as a function of inspection methods and intervals. If the risk is found to be *very small*, this may allow the delaying of certain inspections. Risk-analysis can also be used to evaluate *the effect of aging on the increased risk of operation.* The use of risk-analysis applies a *"systems type approach"* to fatigue life substantiation.

This study compared two very different risk-analysis computer programs to evaluate the risk of increasing inspection intervals for a typical aircraft structure.

PRobability **O**f **F**racture ***(PROF)*** risk-analysis software was developed by the University of Dayton Research Institute (UDRI). ***PROF*** is based solely on crack growth and it establishes the probabilities of failure mathematically.

The principal output of ***PROF*** is the hazard-rate and the probability of failure *since the previous inspection*. The hazard-rate is defined as the probability of failure *during next flight.* The USAF has established hazard-rate criteria as 10^{-7} being a totally acceptable hazard rate. Hazard rate peaks ranging from 10^{-7} to 10^{-5} can be acceptable if their occurrences are limited, while hazard-rates that exceed 10^{-5} are never acceptable.

Another important parameter, the overall probability of failure (from time zero) is not displayed by ***PROF***, but it can be calculated from the individual probabilities of failure that are displayed in the output.

INspection **SIM**ulation ***(INSIM)*** risk-analysis software was developed by IAI. It uses probabilistic (Monte-Carlo) simulations to establish the probability of failure for a specific location. ***INSIM*** considers the crack-initiation life in addition to the crack growth life.

A typical example was risk-analyzed using both ***PROF*** and ***INSIM*** software. The results showed reasonable correlation between both methods of analysis, as is shown in Figure 16.

Risk-analysis was shown to also provide a tool to evaluate the effect of extended service life on the risk of failure, a parameter that is totally absent in the classical damage-tolerance analysis.

The results of this study were presented at the 49th Israel Annual Conference on Aeronautical Sciences [14].

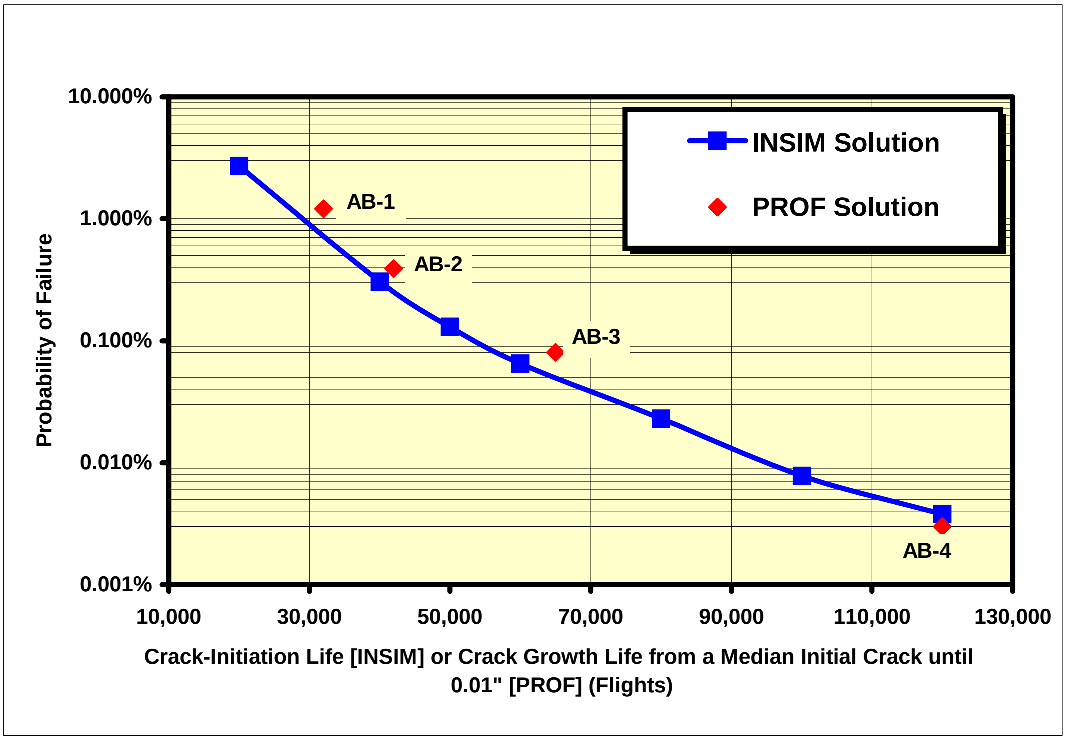

Figure 16: Comparison of Results for Risk-Analyses Performed by *PROF* and *INSIM*

11.4.2 Methodology for Assessing Distribution Characteristics of Crack Growth Data (Y. Rabinowicz and Y. Roman, Hebrew University of Jerusalem)

This study presents a methodology for coping with information loss following consolidation of data on fatigue crack propagation rates derived from different experiments. It is customary to consolidate results of several experiments conducted using identical materials and under similar conditions. This reduces the ability to implement a probabilistic fracture mechanics approach in order to reliably calculate the distribution of the number of cycles needed to reach a critical crack size. Such a calculation requires, among other things, an estimation of the distribution characteristics of the crack progression curves coefficients represented by models such as the Paris or NASGRO equations, and an estimation of the joint-distributions of equation coefficients representing such models. Consolidated data reduce the ability to estimate these required distribution characteristics. Figure 17 is an example of consolidated data used to describe crack-growth characteristics [15].

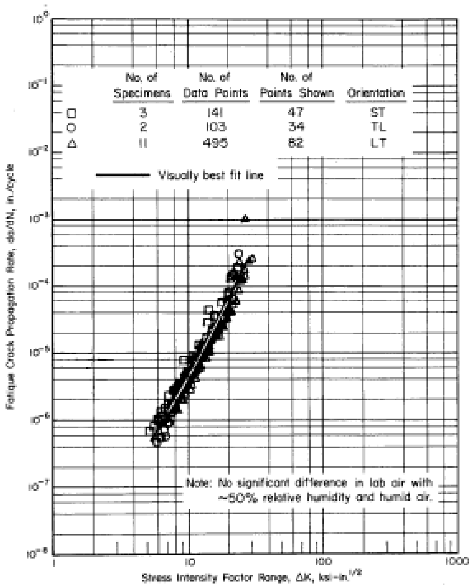

Figure 17: Consolidated Crack-Growth Data for 3.15 inch thick 7050-T7451 Aluminum Plate [15]

This work suggests an analytical approach that uses consolidated data, but enables the information to be treated as if it were possible to attribute the data to the various experimental specimens from which they were obtained. Consequently, information required for the evaluation of the probabilistic distribution of the number of cycles needed to reach a critical crack size can be obtained, as is shown in Figure 18. The proposed method addresses the joint-distribution (using variance and covariance functions) of the equation parameters in order to result the in probabilistic distributions. It has been shown that the failure to consider the joint-distribution may lead to very significant errors.

The proposed approach is generic and can be applied in additional scientific fields that can benefit from separation of data obtained from different experiments.

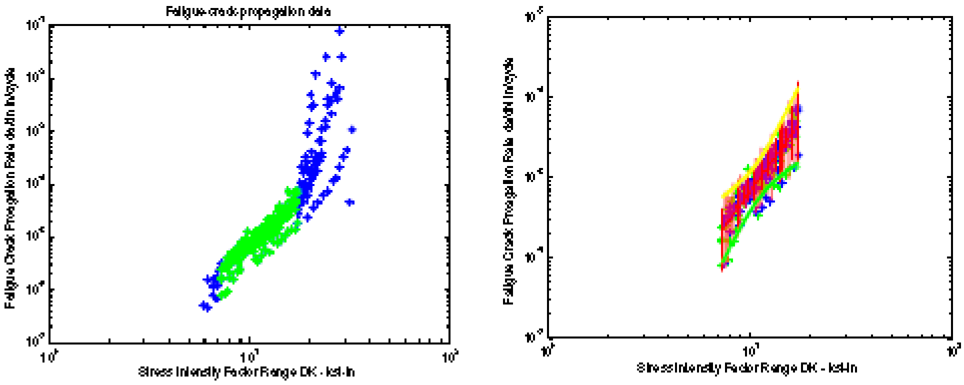

Figure 18: Consolidated da/dN data (left) and its Transformation to Probabilistic Results (right)

11.5 MISCELLANEOUS

11.5.1 Stress-Intensity Functions in the Neighborhood of Edges in a Three-Dimensional Linear Elastic Body (Z. Yosibash, N. Omer, et al, Ben-Gurion University)

This research is a continuation of previous work presented in the 2007 Israel National Review [1].

The computation of eigen-pairs and generalized stress intensity factors in the vicinity of singular points as well as the thermal stress intensity functions in 2-D domains, and their relation to failure initiation is extremely important in engineering practice. Much interest is also devoted to 3-D domains where edge and vertex singularities are present and edge stress intensity functions (ESIFs) in the neighborhood of edges have major importance in engineering practice. These topics are being presented in details with many examples from engineering practice in a new book by Z. Yosibash that is scheduled to appear in 2009 [16].

Elasticity problems in three-dimensional (3-D) polyhedral multi-material anisotropic domains in the vicinity of an edge were also investigated recently by Z. Yosibash [17, 18, 20]. The solution in the vicinity of the edge includes eigen-functions (similar to 2-D domains) complemented by shadow-functions and their associated edge stress intensity functions (ESIFs), which are functions along the edge. These can be complex and are of major engineering importance in composite materials because failure theories directly or indirectly involve them. The p-version finite-element method is used to compute complex eigen-functions and shadows and applied to multi-material anisotropic interfaces. The quasidual function method for extracting edge stress intensity functions is used for extracting complex ESIFs from finite element solutions.

Numerical examples for 3-D isotropic and anisotropic multi-material interfaces are provided for which the complex eigen-pairs and shadow functions are numerically computed and ESIFs extracted. These examples show the efficiency and high accuracy of the numerical approximations. For example, Figure 20 shows the first two ESIFs for a compact tension specimen (Figure 19) having a crack between two composite materials extracted by the proposed methods.

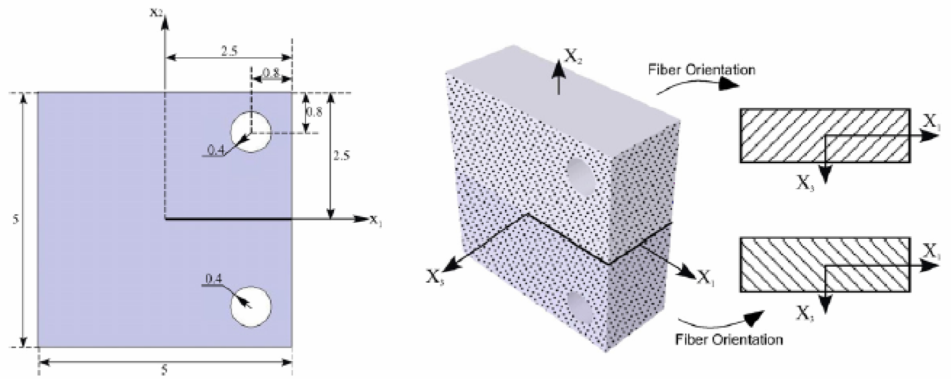

Figure 19: CTS dimensions – with Thickness $-1<x_3<1$

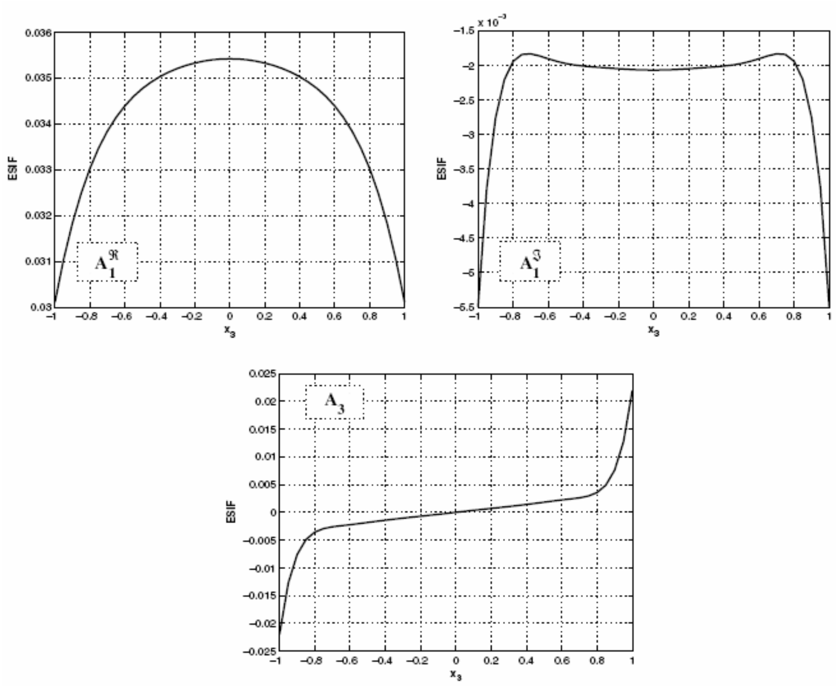

Figure 20: First Complex ESIF (top) and Second ESIF for the CTS Made of Two Composites

11.5.2 Failure Criteria at V-Notched Structures (Z. Yosibash, E. Priel et al, Ben-Gurion University)

This research is a continuation of previous work presented in the 2007 Israel National Review [1].

Another research project [19] is directed to linear elastostatic problems in the vicinity of V-notch ***blunt*** corners subject to mixed mode loading and the formulation of a failure criterion for these problems. A criterion to predict crack onset at a sharp V-notch tip in homogeneous brittle materials under a mixed-mode loading was presented and validated by experimental observations in [21]. This criterion slightly underestimates the experimental loads causing failure which is attributed to a small notch tip radius that blunts the sharp corner. This discrepancy is rigorously analyzed mathematically [19] by means of matched asymptotics involving two small parameters: a micro-crack increment length and the notch tip radius. A correction is brought to the initial prediction and a better agreement is obtained with experiments on PMMA notched specimens. (See Figure 21 & 22.)

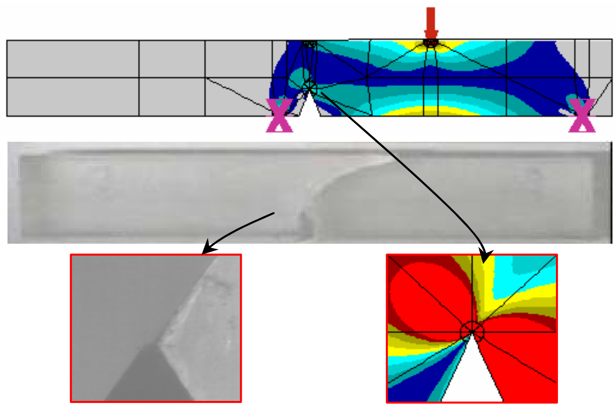

Figure 21: PMMA Specimens Tested and FE Analysis under the Assumption of a Sharp V-notch Tip

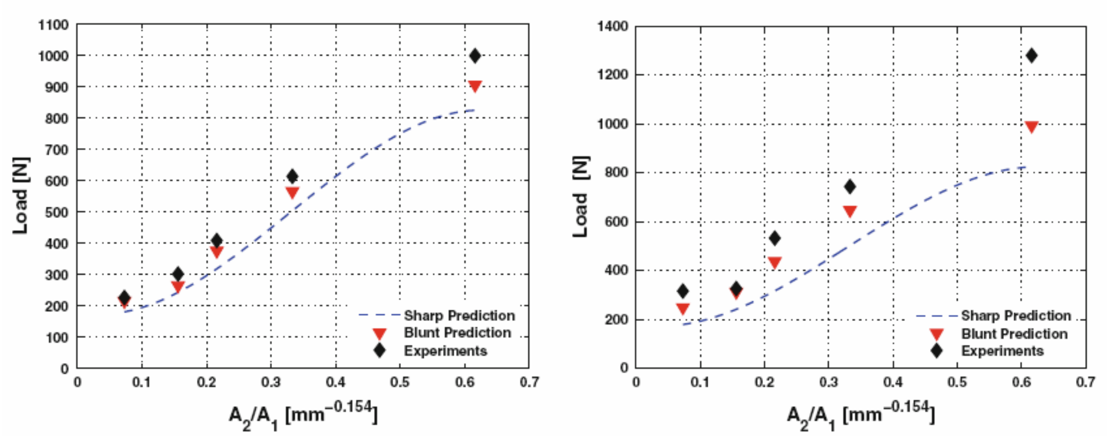

Figure 22: Experimental and Predicted Values for PMMA Specimens under Mixed Mode Loading
(Left— notch tip radius 0.03mm; Right— notch tip radius 0.25mm)

11.5.3 TaxiBot – A New Concept for "Smart" Dispatch Towing (A. Perry and A. Hermelin, IAI)

Since the start of the widespread use of towbarless towing, there have been many suggestions to tow aircraft directly to the takeoff runway (dispatch towing) in order to save fuel and reduce pollution. In the past, these proposals have all been dismissed due to the expected reduction of the fatigue life of the nose landing gear, due to the many towing load cycles that will be applied during dispatch towing [22].

Nevertheless, the dispatch towing concept has many advantages. A study has shown that an annual savings of $8 billion (April 2009 prices) and 18 million tons of CO_2 emission savings can be realized (in 2012), if all wide-body aircraft are towed to their takeoff points. *(A large wide-body aircraft burns about 350 gallons of fuel during the average 22 minute taxi time to reach its takeoff point.)*

IAI is developing a semi-robotic towbarless towing vehicle called TaxiBot. Under this concept, the pilot of the aircraft remains in full command during the entire taxi process. In order to slow down, the pilot will apply the aircraft brakes (on the main landing gears) as needed, thereby reducing the number and magnitude of load cycles applied to the nose gear. The engines will be ignited only shortly before takeoff, thereby saving fuel and reducing pollutants. The TaxiBot control system will be designed to limit the magnitude of loads that can be applied to the nose gear, thereby controlling the towing load spectrum. IAI expects that this approach will not result in any reduction of the nose landing gear fatigue life.

IAI is planning to perform, in coordination with Airbus, a TaxiBot towing demonstration (during December 2009) on an instrumented Airbus 340-600 aircraft. The purpose of this demonstration is to verify the operational performance of the TaxiBot and to confirm that the TaxiBot towing load spectrum is not more severe than the spectrum to which the nose landing gear of the aircraft was certified to.

Figure 23 shows a towbarless vehicle towing a wide-body aircraft. Figure 24 show the design configuration of the TaxiBot vehicle.

Figure 23: Towbarless Vehicle Towing a Wide-Body Aircraft

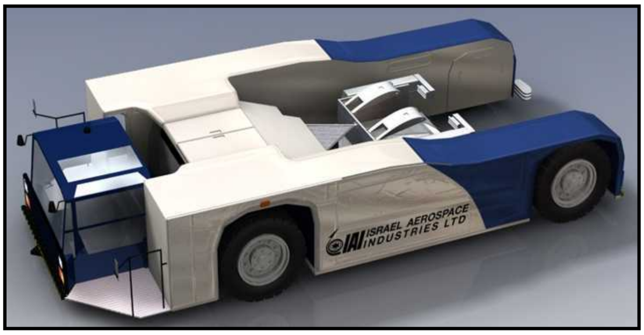

Figure 24: TaxiBot Configuration Including the Clamping System to Secure the Nose Gear

11.5.4 Predictive Maintenance Concepts for Structural Integrity (R. Halevi, IAF)

Predictive maintenance is a *condition based maintenance* program that uses direct monitoring of structural parameters to schedule maintenance activities. This is in contrast to the current practice that uses average life statistics to schedule maintenance. Predictive maintenance has the potential to increase safety and reduce costs. This study traces the use of predictive maintenance concepts in the Israel Air Force (IAF).

The use of predictive maintenance in the IAF is based on installing embedded sensors and the use of recorded flight data. The applicability of MWM, VCM, fiber-optic and piezoelectric sensors was investigated in this study. Crack propagation sensors have been successfully installed under a wing patch repair on an F-16 aircraft about 15 years ago, with successful results.

Building a usage database is another feature of predictive maintenance in the IAF. This database can detect fleet usage changes, allow comparisons of different usage groups, support mishap investigations and allow individual aircraft tracking. Figure 25 shows the use of embedded *Meandering Winding Magnetometer* (MWM) probes to detect cracking on an A-4 aircraft.

The results of this study were presented at the ASIP 2007 Conference [23].

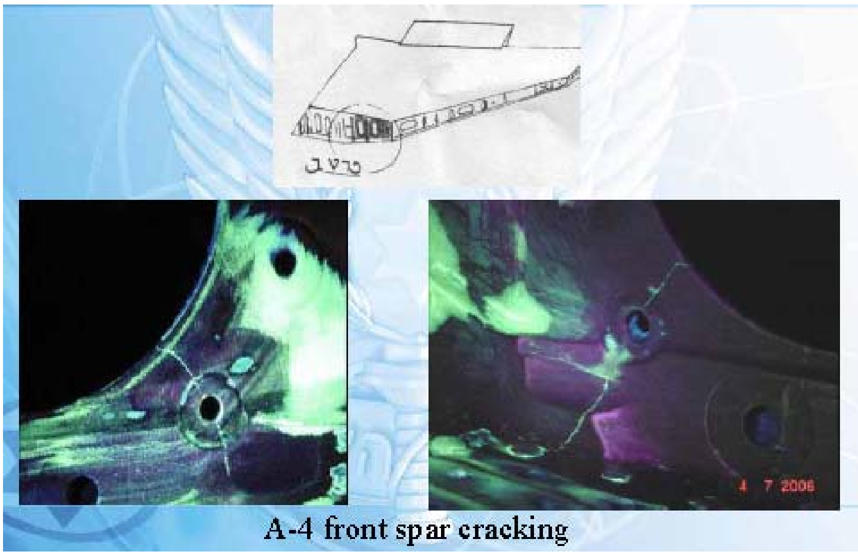

Figure 25: Use of Embedded *Meandering Winding Magnetometer* (MWM) Probes to Detect Cracking

11.5.5 Feasibility Study of MWM Embedded Sensors for Detection & Tracking of Crack Propagation on Flying Aircraft (D. Neuman, IAF)

In a related investigation, the IAF together with JENTEK Sensors Inc., performed a feasibility study for installing MWM *(meandering winding magnetometer)* embedded sensors for crack detection and tracking on a flying aircraft. Coupon tests and environmental tests were performed, in preparation for flight testing.

The MWM-Array developed by JENTEK Sensors, Inc. is a thin foil type gage that operates as an eddy current sensor to detect cracks or as a non-contact stress gage, as is shown in Figure 26. The eddy-current method is not applicable for non-conducting materials, but can work on metals and some composites. The sensors are thin and flexible, which enables one to use them on parts with complex geometry, and install them as embedded sensors in or under structural members of the aircraft.

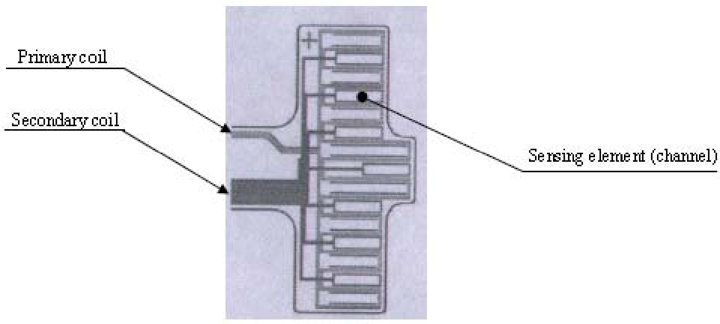

Figure 26: Construction Details of the JENTEK Seven Channel MWM-Array Sensor

The IAF conducted two experiments for evaluating the MWM method before installing the sensors on airplanes. The first experiment was a coupon test. The purpose of this test was to check if the MWM system could track the crack growth.

This test included two separate procedures, in the first procedure the system was working continuously and monitored the crack until specimen's failure, as is shown in Figure 27.

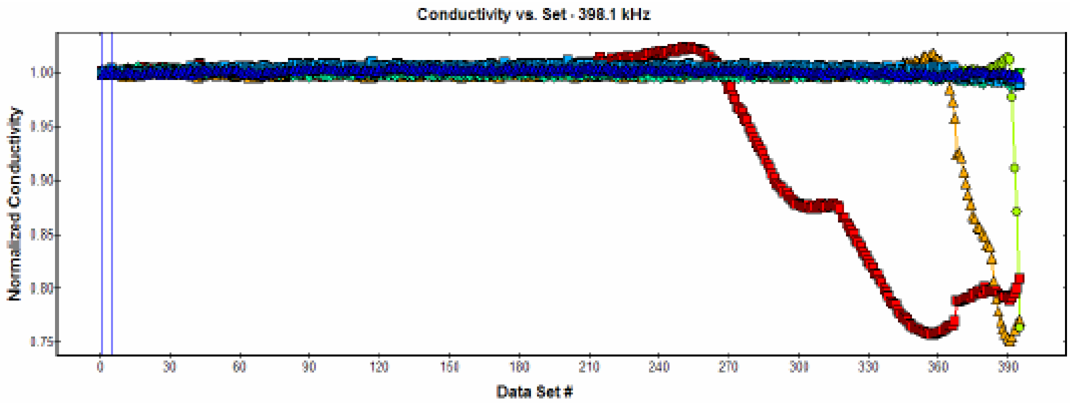

Figure 27: Crack Growth Measurements under Continuous Operation

In the second procedure, the specimen was loaded for a period of time, then load was removed and the MWM system was connected in order to record the crack response. Then the MWM system was disconnected and the specimen was loaded again for another discrete period of time. This was repeated throughout the test. This experiment lasted until failure of the specimen. The purpose of the second procedure of the coupon test was to verify performance in the same format intended on-aircraft, i.e., with the system plugged-in periodically to record the data. The results of the testing were positive.

The second experiment was a vibration test: in this test the sensor was located on a cracked aluminum specimen and under a steel plate. 18g (rms) vibrations were then applied for each direction**.** The sensors survived the vibration testing.

After conducting these experiments, the next phase was to install the sensors on a flying aircraft. The IAF chose to install sensors on the forward spar of the A-4 wing on a crack growing from the elliptic hole (see Figure 25). A repair was designed for this location to allow safe flight and adequate service life. However, the crack growth direction was unknown, since the crack may grow in two possible paths. The first path is on the web until the radius between the web and the lower cap and then on the radius in the outboard direction. The second path is on the web until the radius between the web and the cap and then on the cap in forward direction until it reaches one of the holes placed on the cap.

After conducting a fatigue analysis, the probability of the second path described above was found to be greater than the first path. Despite this analysis, two sensors will be installed to cover both options. The purpose of the experiment is to examine the effect of flight on the measurements and to evaluate the ability of the MWM-Array method to detect cracks and to monitor the crack growth. After installation on the aircraft, the sensors will be monitored periodically. The repair will be disassembled after 50, 125 and 250 flight hours for inspection of the cap. Sensor readings will be compared with actual findings. Upon a successful conclusion of flight tests, the IAF will consider extending the use of MWM sensors to other locations and platforms.

The results of this study were presented at the 49th Israel Annual Conference on Aeronautical Sciences [24].

11.5.6 Interface Cracks in Fiber Reinforced Composites (L. Banks-Sills, Tel-Aviv University)

During the last two years, characterization of the behavior of interface cracks between fiber reinforced, laminate composite material has been continuing. Two graduate students have been carrying out investigations on 0°/90°, 90°/0°, +30°/-60° and -30°/60° interfaces.

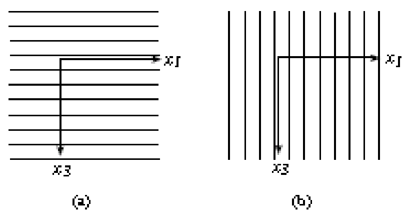

Figure 28: (a) Fibers in the Upper Material are in the x_1-Direction, Whereas (b) Fibers in the Lower Material in the x_3-Direction

For example, for the 0°/90° interface, the fibers of the composite of the upper material are in the x_1-direction (see Fig. 28a), whereas the fibers in the lower material are in the x_3-direction (see Fig. 28b). The other material pairs are defined in a similar manner with a positive sign indicating rotation clockwise from the x_1-axis. The delamination is situated in the $x_1 - x_3$ plane (see Fig. 29) with the x_3-axis along the delamination front and the x_2-axis perpendicular to the delamination faces.

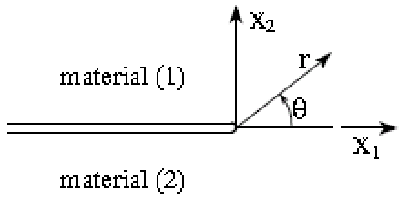

Figure 29: Delamination Front Coordinates

Banks-Sills and Boniface [25] derived the first term of the asymptotic solution for the stress and displacement fields for the 0°/90° interface. It was found that the in-plane stresses in the neighborhood of the delamination front behave as,

$$\sigma \sim \left\{ \begin{array}{l} \frac{1}{\sqrt{r}} \cos(\varepsilon \ln r) \\ \frac{1}{\sqrt{r}} \sin(\varepsilon \ln r) \end{array} \right.$$

where r is the distance from the delamination front (see Fig. 29) and ε, the oscillatory parameter, is a function of the effective mechanical properties of the two materials. The same behavior seen in the above equation is found for an interface crack between two isotropic materials. The major differences are in the form of the oscillatory parameter ε and the expressions for the stresses and displacements. As part of their investigation, they extended a conservation integral, the *M*-integral for calculating stress intensity factors for this case.

Alperovitch [26] re-examined their solution, considering the effect of the sign of ε. It was observed that the same expressions are found with ε replaced with -ε, $K_1^{\varepsilon<0} = -K_1^{\varepsilon>0}$ and $K_2^{\varepsilon<0} = K_2^{\varepsilon>0}$; the superscript denotes the sign of ε and the in-plane complex stress- intensity factor is given by $K = K_1 + iK_2$ where $i = (-1)^{1/2}$ and K_1 and K_2 are the modes 1 and 2 stress intensity factors, respectively. Alperovitch [26] continued by developing the first term of the asymptotic expressions for the 90°/0°interface. These were used to extend the *M*-integral for this case. Finally, a square delamination in a cross-ply laminate was examined (see Fig. 30). Using test results obtained in [27], it is predicted that the delamination is weakest at the center of each delamination front when tension is applied perpendicular to the crack faces on the outer edge of the cross-ply. When in-plane shear is applied, the 0°/90° interfaces are weakest (along sides AB and CD). Applied tension was found to be much more dangerous than applied shear.

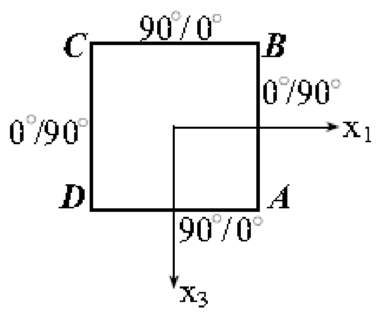

Figure 30: Square Delamination in a Cross-Ply Laminate

This work was extended in [28] to an octagonal delamination as shown in Fig. 31. Along the sides AB and EF, the interface is 0°/90°; along CD and GH, it is 90°/0°; along BC and FG, it is +45°/-45°; and along DE and HA, it is -45°/+45°. It was found that when the cross-ply is subjected to tension perpendicular to the crack faces, edges AB, CD, EF and GH are weak. For in-plane shear, sides AB and EF, namely, the 0°/90° interfaces are the weakest. Applied tension was found to be much more dangerous than applied shear.

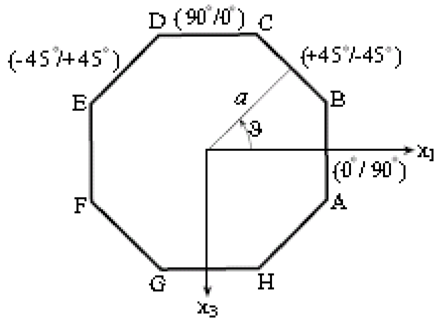

Figure 31: Octagonal Delamination in a Cross-Ply Laminate

Continuing these studies, Rogel [29] is developing the asymptotic fields for the +30°/-60° and -30°/60° interfaces. In these cases, as well as most others, there are five stress-intensity factors, namely K_1, K_2 and K_3 associated with the square-root, oscillatory singularity and K_{II} and K_{III} associated with the square-root singularity. It was found, however, that there is a relation between K_2 and K_3, as well as between K_{II} and K_{III}. Tests are planned for the +30°/-60° interface. These studies are leading up to an investigation of a penny-shaped crack in a cross-ply.

11.5.7 Cracks in Shape Memory Alloys (L. Banks-Sills, Tel-Aviv University)

Another area of interest has been the investigation of cracks in shape memory alloys (SMAs). In the first study [30], the transformation toughening behavior of a slowly propagating crack in an SMA under plane-strain conditions and mode I deformation was numerically investigated. A small-scale transformation zone was assumed. A cohesive zone model was implemented to simulate crack growth within a finite-element scheme. Resistance curves were obtained for a range of parameters that specify the cohesive traction-separation constitutive law. It was found that the choice of the cohesive strength t_0 has a great influence on the toughening behavior of the material. Moreover, the reversibility of the transformation can significantly reduce the toughening of the alloy. The shape of the initial transformation zone, as well as that of a growing crack was determined. The effect of the Young's moduli ratio of the martensite and austenite phases was examined.

In [31], a bilinear cohesive zone model was employed to describe the transformation toughening behavior of a slowly propagating crack along an interface between a shape memory alloy and a linear elastic or elasto-plastic isotropic material. Small scale transformation zones and plane-strain conditions were assumed. The crack growth was numerically simulated within a finite-element scheme and its transformation toughening was obtained by means of resistance curves. It was found that the choice of the cohesive strength t_0 and the stress-intensity factor phase angle ϕ greatly influence the toughening behavior of the bimaterial. The presented methodology was generalized for the case of an interface crack between a fiber reinforced shape memory alloy composite and a linear elastic, isotropic material. The effect of the cohesive strength t_0, as well as the fiber volume fraction were examined.

In addition, a new two-dimensional cohesive zone model, which is suitable for the prediction of mixed mode interface fracture in bimaterials, was presented in [32]. The model accounts for the well known fact that the interfacial fracture toughness is not a constant, but a function of the mode mixity. Within the framework of this model, the cohesive energy and the cohesive strength were not chosen to be constant, but rather functions of the mode mixity. A polynomial cohesive zone model was derived in light of analytical and experimental observations of interface cracks. The validity of the new cohesive law was examined by analyzing double cantilever beam and Brazilian disk specimens. The methodology to determine the parameters of the model was outlined and a failure criterion for a pair of ceramic clays was suggested.

11.5.8 Stress-Intensity Factors for Cracks in Piezoelectric Materials (L. Banks-Sills, Tel-Aviv University)

Studies on the cracking of piezoelectric materials are in progress. The conservative *M*-integral was extended for calculating intensity factors for cracks in piezoelectric materials with impermeable [33] and exact [34] boundary conditions. There are four intensity factors for cracks in piezoelectric materials: the usual stress-intensity factors for the three modes of deformation K_I, K_{II} and K_{III} and a fourth intensity factor K_{IV} related to the electric flux density vector *Di*. Motola has recently submitted a Ph.D. thesis [35]. In that investigation, tests were carried out on cracked PZT-5H poled parallel to the crack faces. An energy based fracture criterion was developed which was used to describe these test results with fairly good agreement observed. In addition, test results obtained by

Jellito et al. [36], in which the crack was perpendicular to the poling direction, were analyzed. The test results were in excellent agreement with the fracture criterion.

11.6 REFERENCES

1. Brot, A., “Review of Aeronautical Fatigue Investigations in Israel, April 2005 – March 2007”, *Minutes of the 30th ICAF Conference,* Naples, Italy, 2007.

2. Brot, A., and Matias, C., "Residual Tensile Stresses Induced by Cold-Working a Nearby Fastener Hole", *Proceedings of the 47th Israel Annual Conference on Aerospace Sciences*, 2007.

3. Brot, A., and Matias, C., "The Effects of Residual Tensile Stresses Induced by Cold-Working a Fastener Hole", *Proceedings of the USAF Aircraft Structural Integrity Program Conference*, 2007.

4. Perl, M., "Thermal Simulation of an Arbitrary Residual Stress Field in a Fully or Partially Autofrettaged Thick-Walled Pressure Vessel", *Journal of Pressure Vessel Technology*, Vol. 130, 2008.

5. Levy, C., Perl, M. and Kotagiri, S., "The Combined Stress Intensity Factors of Multiple Longitudinally Coplaner Cracks in Autofrettaged Pressurized Tubes Influenced by the Bauschinger Effect", *Journal of Pressure Vessel Technology*, Vol. 130, 2008.

6. Ma, Q., Levy, C. and Perl, M., "The Bauschinger Effect on 3-D SIFs for Networks of Radial and Longitudinaly-Coplaner Semi-Elliptical Surface Cracks in Autofrettaged Pressurized Thick-Walled Cylinders", *CMES*, vol. 29, no. 2, 2008.

7. Perry, J. and Perl, M., "A 3-D Model for Evaluating the Residual Stress Field due to Swage Autofrettage", *Journal of Pressure Vessel Technology*, Vol. 130, 2008.

8. Granot, Z., “Simplified Methods for Predicting Fatigue Life of Composite Material Structures”, *Proceedings of the 23rd ICAF Symposium*, 2005.

9. Kressel, I et al., "Damage Tolerance of Bonded Composite Repairs – Analysis and Tests”, *Proceedings of the 23rd ICAF Symposium*, 2005.

10. Kressel, I et al., "Smart Bonded Composite Patch Repairs – Analysis and Testing", *Proceeding of the 24th ICAF Symposium*, 2007.

11. Brot, A., Peleg-Wolfin, Y., Kressel, I. and Yosef, Z., "The Damage-Tolerance Behavior of Integrally Stiffened Metallic Structures", *Proceedings of the 48th Israel Annual Conference on Aerospace Sciences,* 2008.

12. Brot, A., Peleg-Wolfin, Y., Kressel, I. and Yosef, Z., "The Use of Composite Material Strips to Extend the Damage-Tolerance Life of Integrally Stiffened Aluminum Panels", *Proceedings of the 25th ICAF Symposium,* 2009.

13. Kressel, I., "Substantiations of an Airborne Composite Radome Mounted on an Aircraft Dome", *Proceedings of the 25th ICAF Symposium,* 2009.

14. Brot, A., "Risk-Analysis – a Supplement to Damage-Tolerance Analysis", *Proceedings of the 49th Israel Annual Conference on Aerospace Sciences,* 2009.

15. MIL-HDBK-5J, *USAF*, 2003.

16. Yosibash Z., "Singularities in Elliptic Boundary Value Problems and Elasticity and their Connection with Failure Initiation", Springer, to be published in 2009.

17. Omer N. and Yosibash Z., "Edge Singularities in 3-D Elastic Anisotropic and Multi-Material Domains", *Computer Methods in Applied Mechanics and Engineering,* vol. 197, 2008.

18. Yosibash Z., Omer N. and Dauge M., "Edge Stress Intensity Functions in 3-D Anisotropic Composites", *Composites Science and Technology*, vol. 68, 2008.

19. Priel E., Yosibash Z. and Leguillon, D., "Failure Initiation at a Blunt V-Notch Tip under Mixed Mode Loading", *International Journal of Fracture*, vol. 149, 2008.

20. Apel T., Leguillon D., Pester C. and Yosibash Z., "Edge Singularities and Structure of the 3-D Williams' Expansion", Comptes Rendus Mecanique - Acad. Sci. Paris, vol. 336, 2008.

21. Priel E., Bussiba A., Gilad I. and Yosibash Z.,"Mixed Mode Failure Criteria for Brittle Elastic V-Notched Structures", *International Journal of Fracture*, vol. 144, 2007.

22. Buxbaum, O., Cuny, J.J., Klatschke, H. and Steinhilber, H., "Loads at the Nose Landing Gear of Civil Transport Aircraft During Towbarless Towing Operations", *Proceedings of the 16th ICAF Symposium,* 1991.

23. Halevi, R., "Using Predictive Maintenance Concepts for Structural Integrity in the IAF", *Proceedings of the USAF Aircraft Structural Integrity Program Conference*, 2007.

24. Goldfine, N., Grundy, D., Gruszkeiwicz, D., Neuman, D. and Levi, K., "IAF Feasibility Study of MWM Embedded Sensors for Detection and Tracking of Crack Propagation", *Proceedings of the 49th Israel Annual Conference on Aerospace Sciences,* 2009.

25. Banks-Sills, L. and Boniface, V., "Fracture Mechanics for an Interface Crack Between a Special Pair of Transversely Isotropic Materials", in: *Multiscale Deformation and Fracture in Materials and Structures–The James R. Rice 60th Anniversary Volume*, eds. T.-J. Chuang and J.W. Rudnicki, Kluwer Academic Publishers, The Netherlands, 2000.

26. Alperovitch, A., "Stress Intensity Factors for a Square Delamination in a Cross-Ply Composite", M.Sc. Tel Aviv University, submitted 2009.

27. Banks-Sills, L., Boniface, V. and Eliasi, R., "Development of a Methodology for Determination of Interface Fracture Toughness of Laminate Composites–the 0°/90° Pair". *International Journal of Solids and Structures,* **42**, 2005.

28. Banks-Sills, L., Freed, Y. and Alperovitch, A., "Behavior of a Flat Internal Delamination Within a Fiber Reinforced Cross-Ply Composite", to appear: *International Journal of Fracture*, 2009.

29. Rogel, L., "A Through Interface Crack Between a Transversely Isotropic Pair of Materials: +30°/-60°", M.Sc., Tel Aviv University, in progress.

30. Freed, Y., and Banks-Sills, L., "Crack Growth Resistance of Shape Memory Alloys by Means of a Cohesive Zone Model", *Journal of the Mechanics and Physics of Solids,* **55**, 2007.

31. Freed, Y. and Banks-Sills, L., "A New Cohesive Zone Model for Mixed Mode Interface Fracture in Bimaterials", *Engineering Fracture Mechanics*, **75**, 2008.

32. Freed, Y., Banks-Sills, L. and Aboudi, J., "On the Transformation Toughening of a Crack Along an Interface Between a Shape Memory Alloy and an Isotropic Medium", *Journal of the Mechanics and Physics of Solids*, **56**, 2008.

33. Banks-Sills, L., Motola, Y. and Shemesh, L., "The M-integral for Calculating Intensity Factors of an Impermeable Crack in a Piezoelectric Material", *Engineering Fracture Mechanics*, **75**, 2008.

34. Motola, Y. and Banks-Sills, L., "M-Integral for Calculating Intensity Factors of Cracked Piezoelectric Materials using the Exact Boundary Conditions", Journal of Applied Mechanics, 76, 2009.

35. Motola, Y., "Problems in Fracture Mechanics of Piezoelectric Ceramics – Analytical, Numerical and Experimental Analyses", Ph.D., Tel Aviv University, submitted 2009.

36. Jellito, H., Kessler, H., Schneider, G. A. and Balke, H., "Fracture Behavior of Poled Piezoelectric PZT under Mechanical and Electrical Loads", *Journal of the European Ceramic Society*, **25**, 2005.